



Supplemental Material to:

Hai-Xin Yuan, Ryan Russell, Kun-Liang Guan

**Regulation of PIK3C3/VPS34 complexes by MTOR
in nutrient stress-induced autophagy**

Autophagy 2013; 9(12)

<http://dx.doi.org/10.4161/auto.26058>

www.landesbioscience.com/journals/autophagy/article/26058

Supplemental figures

Figure S1

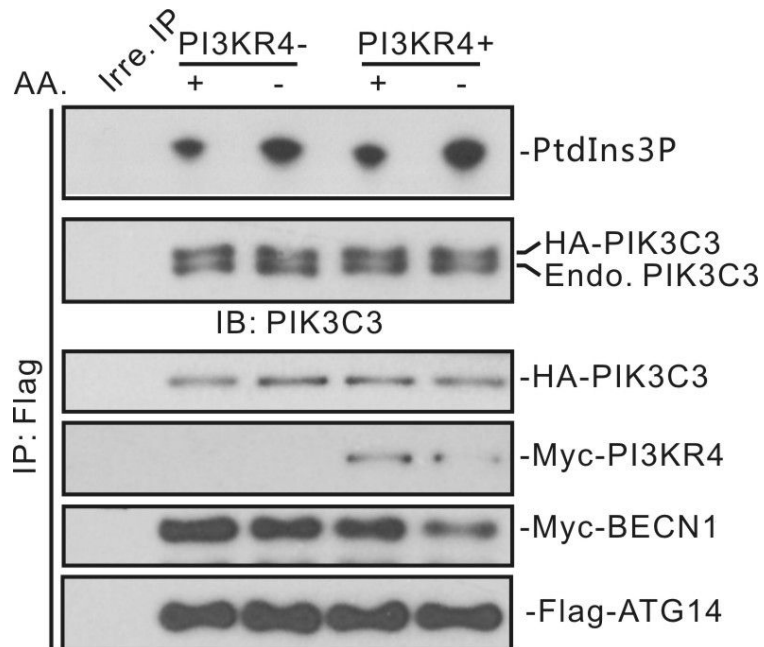


Figure S1. Epitope tagged PIK3C3 expressed at a level similar to endogenous protein is able to be fully activated by endogenous PI3KR4. Coexpression of PI3KR4 does not further increase PIK3C3 activity.

Figure S2

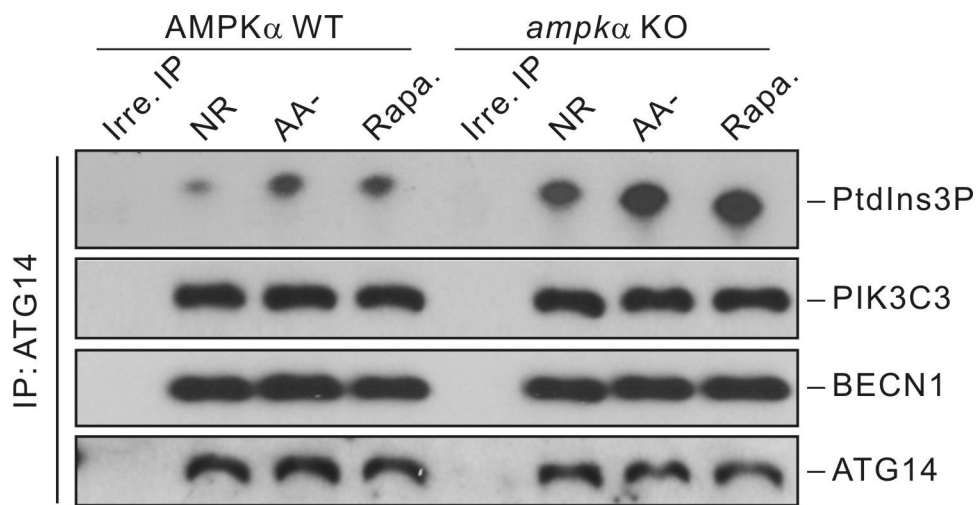


Figure S2. AMPK is not required for ATG14-PIK3C3 activation by amino acid starvation. AMPK α WT or KO MEFs were deprived of amino acids or treated with rapamycin (50nM) for one hour and subjected to lipid kinase assay.

Figure S3

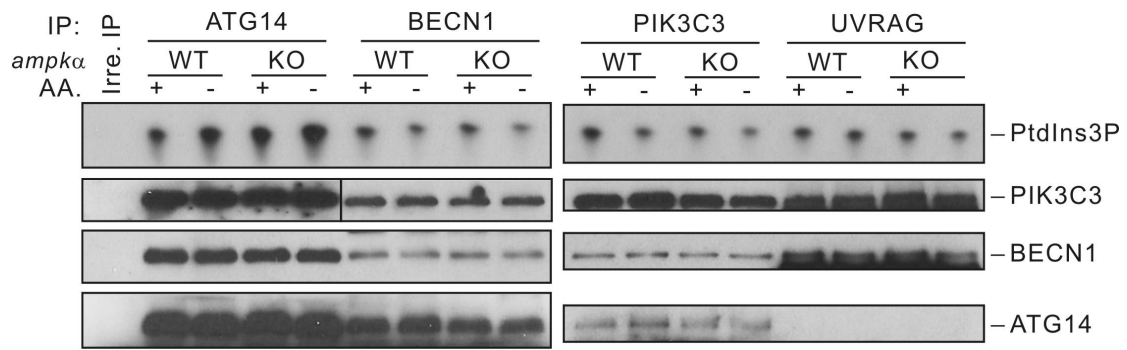


Figure S3. AMPK is not involved in the regulation of different PIK3C3 complexes in response to nutrient condition change. Different PIK3C3 complexes were immunoprecipitated from AMPK α WT or KO MEFs under nutrient-rich or amino acid-free conditions, and subjected to lipid kinase assay.

Figure S4

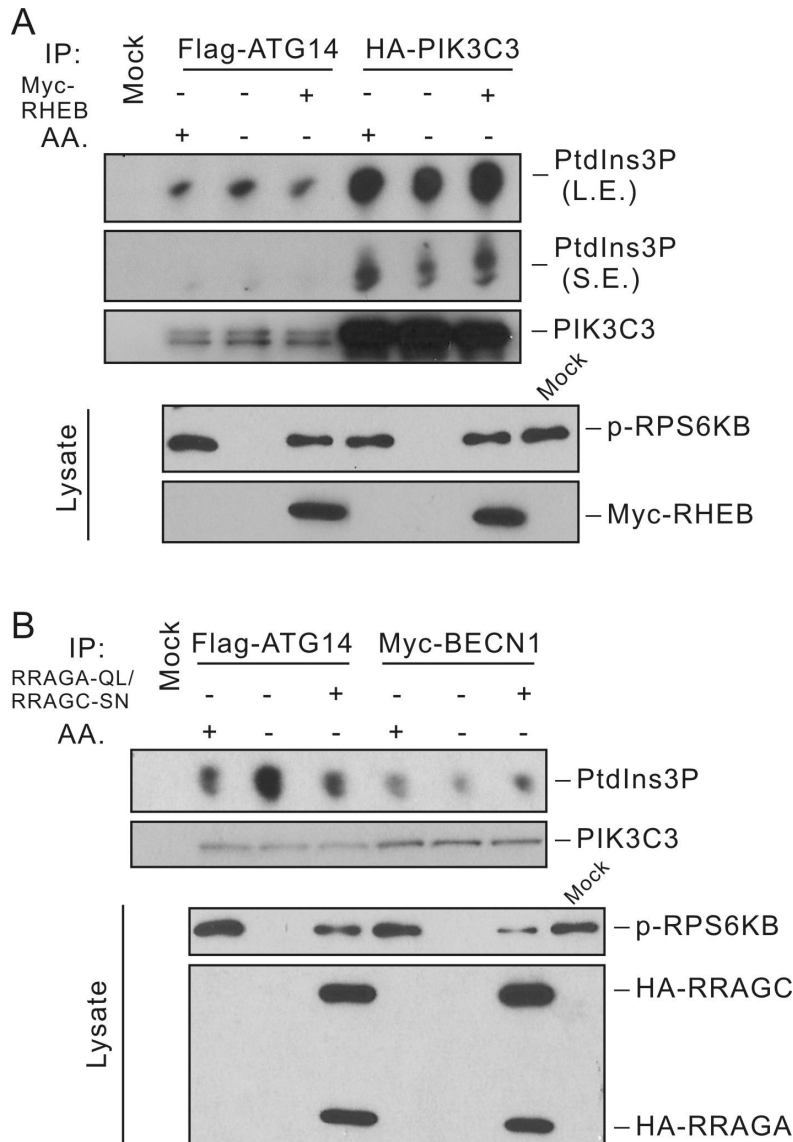


Figure S4. Different PIK3C3 complexes are differentially regulated by MTORC1 signaling. **(A)** RHEB inhibits ATG14-PIK3C3 even in the absence of amino acids. HEK293 cells were cotransfected with Flag-ATG14, Myc-BECN1 and HA-PIK3C3 together with Myc-RHEB. Different PIK3C3 complexes were immunoprecipitated with the indicated antibodies and subjected to lipid kinase assay. **(B)** Active Rag GTPases inhibit ATG14-PIK3C3. Experiments were similar to **(A)** except HA-RRAGA-QL/HA-RRAGC-SN was used in the transfection.

Figure S5

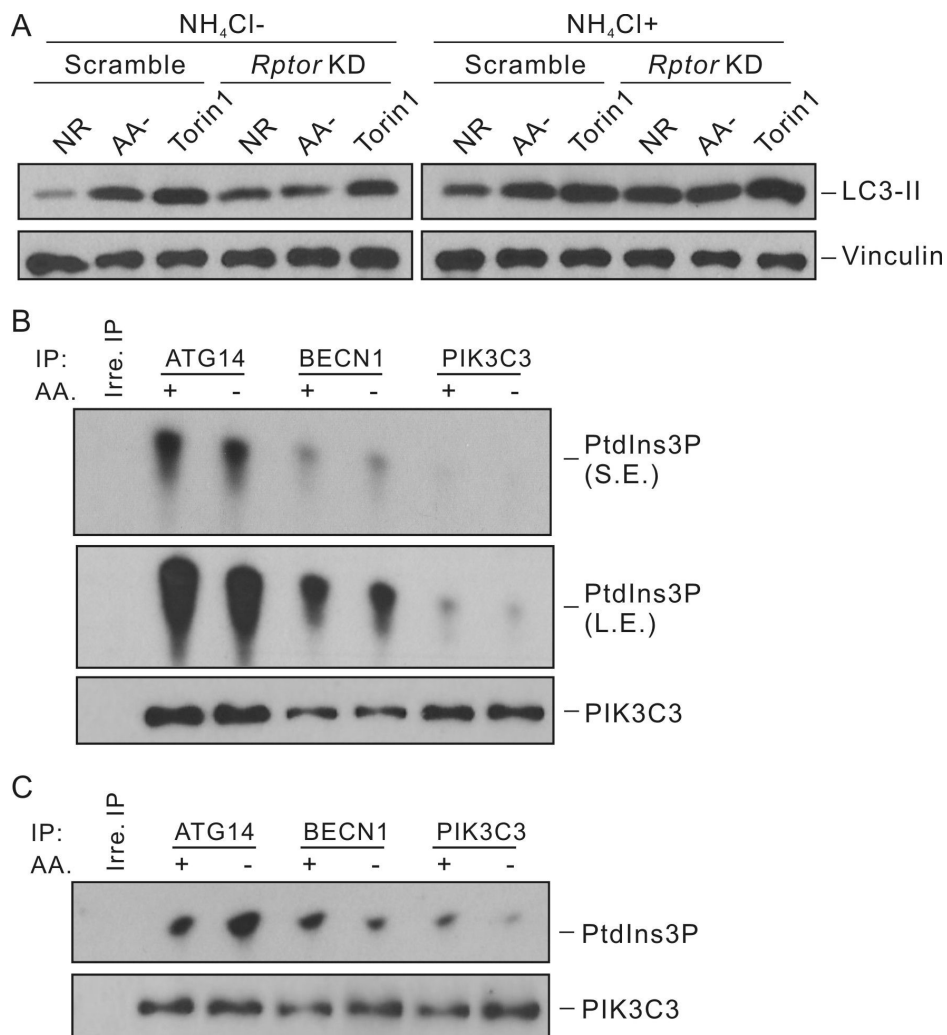


Figure S5. MTORC1, but not MTORC2, regulates PIK3C3 complexes and autophagy. (A) Knockdown of *Rptor* resulted in an increase of basal autophagy flux. Scrambled or *Rptor* KD MEFs were subjected to amino acid starvation or Torin1 (100 nM) treatment for one hour. LC3 levels were detected by immunoblot. (B) Different PIK3C3 complexes were immunoprecipitated from *Rptor* KD MEFs that were cultured in nutrient-rich or amino acid-free medium for one hour, and subjected to lipid kinase assay. (C) Different PIK3C3 complexes were immunoprecipitated from *rictor* KO MEFs that were cultured in nutrient-rich or amino acid-free medium for one hour, and subjected to lipid kinase assay.

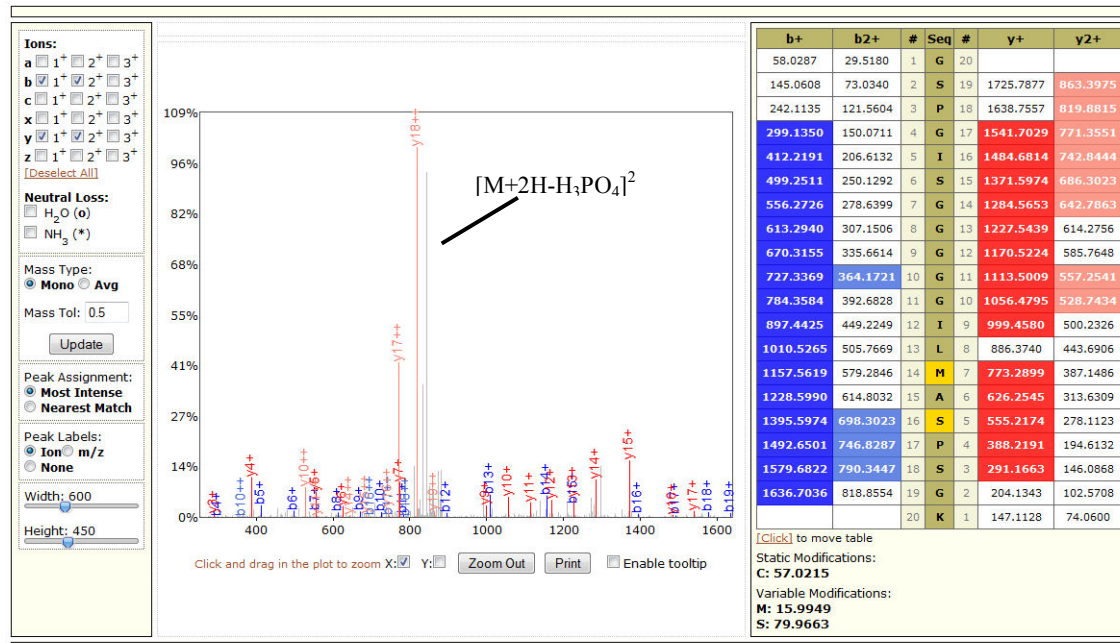
Figure S6

Summary of phosphosite identification in ATG14:

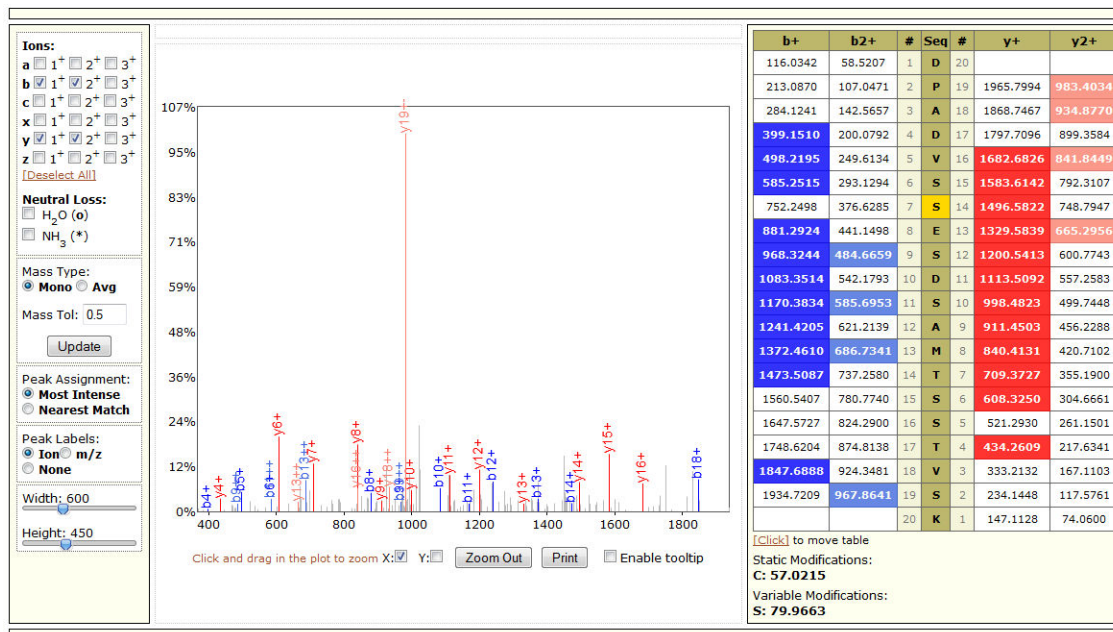
Panel Label ^a	Phosphosite Location	Sequence ^b	Charge State	Absolute Mass Deviation ^c	Peptide Prophet Error Rate
A	S240	GSPGISGGGGIL(oM)A(pS)PSGK	+2	1.3 ppm	5%
B	S460	DPADV(pS)ESDSAMTSSTVSK	+2	2.1 ppm	3%
C	T470	DPADVSESDSA(oM)TSS(pT)VSK	+2	1.8 ppm	1%
D	S620	NL(oM)YLV(pS)PSSEHLGR	+2	2.3 ppm	4%
E	S677	VSDEETDLGTDWENLP(pS)PR	+2	3.7 ppm	0%

- a) Panel labels from figure S8.
- b) “oM”, “pS”, and “pT” correspond to oxidized methionine, phosphoserine, and phosphothreonine.
- c) Corresponds to the absolute value of the difference between the experimentally measured peptide mass and the calculated peptide mass.

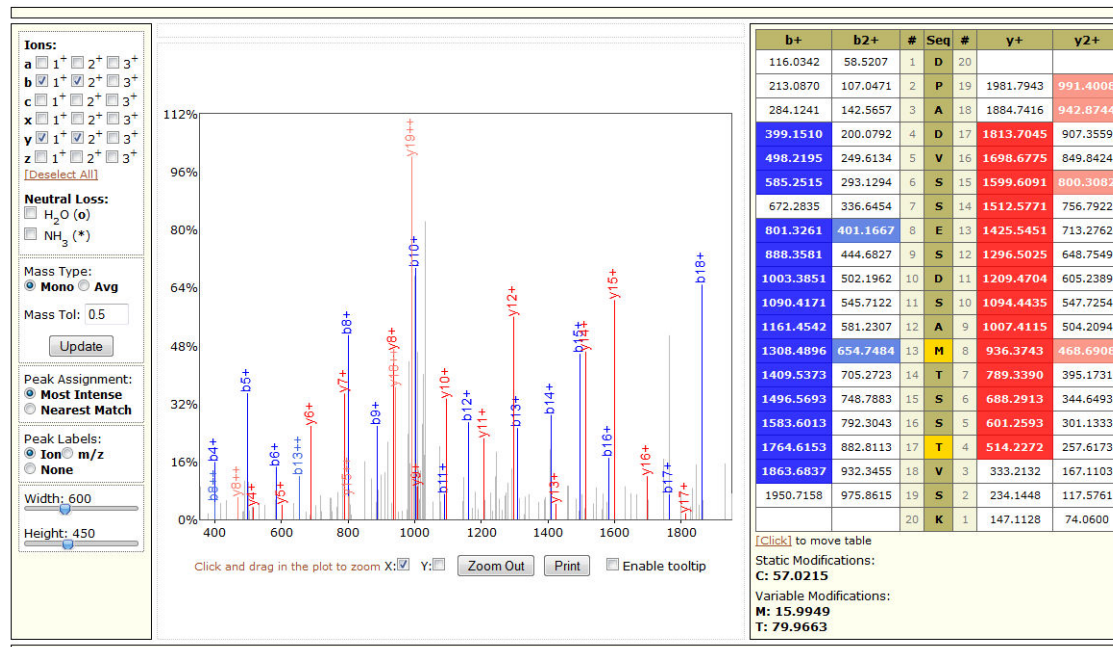
A. Identification of S240



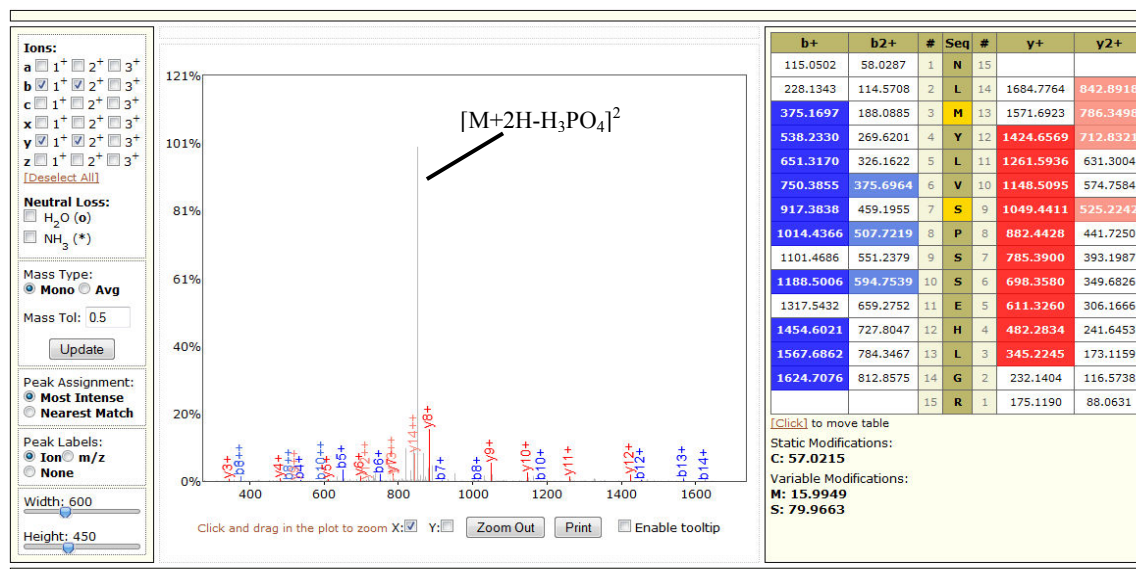
B. Identification of S460



C. Identification of T470



D. Identification of S620



E. Identification of S677

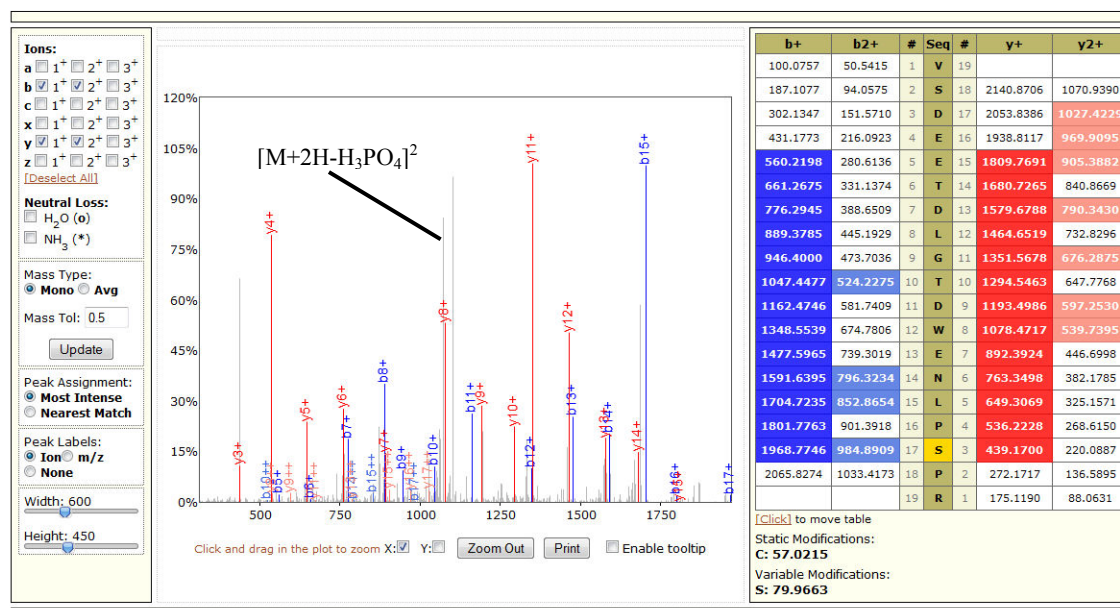


Figure S6. Mass spectrometric identification of phosphosites within ATG14-GST. A gel band corresponding to ATG14-GST fusion protein was cut from a SDS-PAGE gel after an in vitro kinase reaction. The gel band was subjected to in-gel trypsin digestion and the resulting peptide mixture was subjected to liquid chromatography coupled to tandem mass spectrometry (LC-MS/MS). Protein and modification identification were performed with the database search algorithm X!Tandem and peptide identifications were validated with Peptide Prophet. Database search results identified five phosphorylation sites (panels A through E) within four tryptic peptides of ATG14. Each panel shows the recorded tandem mass spectrum and the mass peaks within the

spectrum that match to theoretical b-ions (blue) and y-ions (red); a mass peak corresponding to the loss of phosphoric acid (H_3PO_4), a common occurrence in tandem mass analysis of phosphopeptides, is manually labeled in some panels. The amino acid sequences of the identified phosphopeptides are also displayed along with their theoretical fragment ions. Those fragments that were observed in the tandem mass spectrum are highlighted in blue for b-ions and red for y-ions. The combination of low mass deviation, low Peptide Prophet error rate, and high percentage of theoretical b- and y-ions matching to those ions in the tandem mass spectrum (Figure S8) resulted in these identifications being considered as high confidence phosphosite identifications.

Figure S7

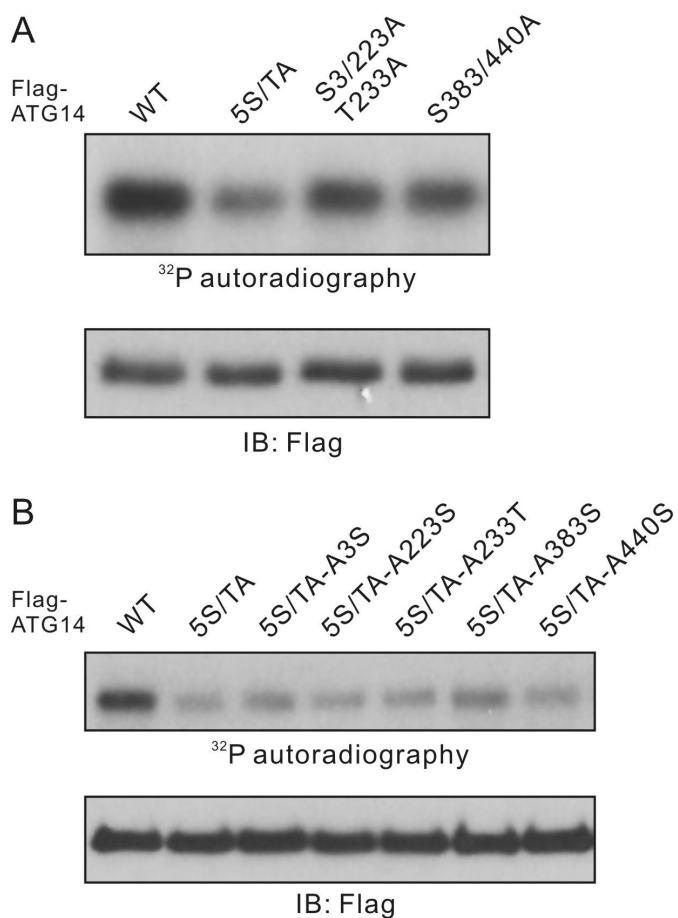


Figure S7. MTOR phosphorylates ATG14 at multiple sites. **(A)** Mutation of the first three sites (Ser3, Ser223 and Thr233) or last two sites (Ser383 and Ser440) partially prevented ATG14 phosphorylation by MTOR. **(B)** Reversion of any of the alanine residues back to serine or threonine could not fully restore the phosphorylation of ATG14 by MTOR.

Figure S8

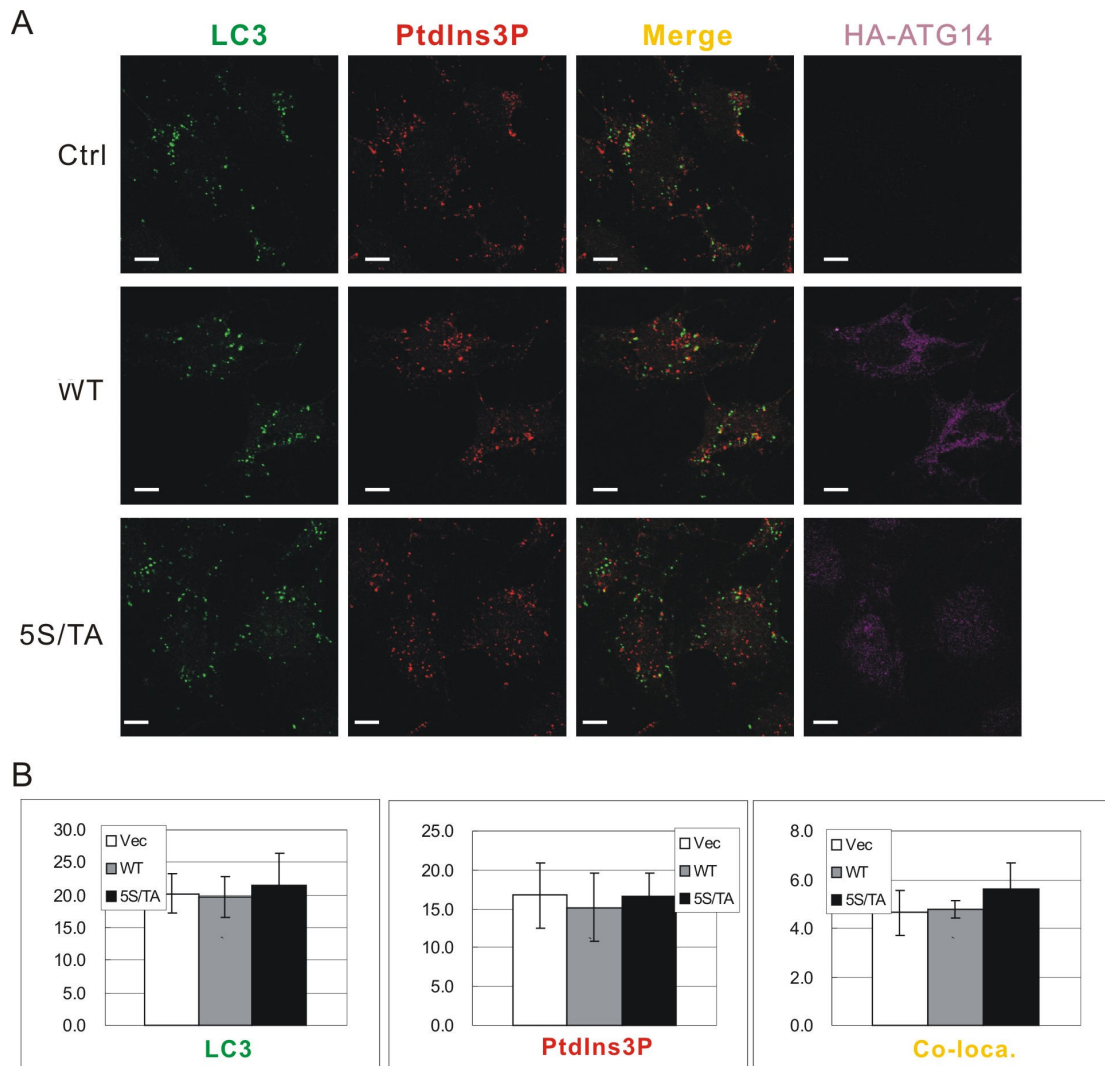


Figure S8. Overexpression of ATG14-WT or ATG14-5S/TA resulted in similar LC3 puncta formation and colocalization of LC3 and PtdIns3P under amino acid starvation conditions. **(A)** HEK293A cells stably expressing control vector, ATG14-WT or ATG14-5S/TA were cultured in AA-free medium for one hour. Cells were fixed and subjected to immunostaining with a GST-FYVE probe and antibodies against HA and LC3. Scale bar: 10 μ m. **(B)** Quantification of the staining in **(A)**.